University of Nebraska - Lincoln

DigitalCommons@University of Nebraska - Lincoln

6-2012

Multifunctional CD4 Cells Expressing Gamma Interferon and Perforin Mediate Protection against Lethal Influenza Virus Infection

Deborah M. Brown
University of Nebraska-Lincoln, dbrown7@unl.edu

Sarah Lee
University of Nebraska-Lincoln

Maria de la Luz Garcia-Hernandez
University of Nebraska-Lincoln

Susan L. Swain
University of Nebraska-Lincoln, susan.swain@umassmed.edu

Multifunctional CD4 Cells Expressing Gamma Interferon and Perforin Mediate Protection against Lethal Influenza Virus Infection

Deborah M. Brown, Sarah Lee, Maria de la Luz Garcia-Hernandez,* and Susan L. Swain*

School of Biological Sciences, Nebraska Center for Virology, University of Nebraska—Lincoln, Lincoln, Nebraska, USA

CD4 effectors generated *in vitro* can promote survival against a highly pathogenic influenza virus via an antibody-independent mechanism involving class II-restricted, perforin-mediated cytotoxicity. However, it is not known whether CD4 cells activated during influenza virus infection can acquire cytolytic activity that contributes to protection against lethal challenge. CD4 cells isolated from the lungs of infected mice were able to confer protection against a lethal dose of H1N1 influenza virus A/Puerto Rico 8/34 (PR8). Infection of BALB/c mice with PR8 induced a multifunctional CD4 population with proliferative capacity and ability to secrete interleukin-2 (IL-2) and tumor necrosis factor alpha (TNF-α) in the draining lymph node (DLN) and gamma interferon (IFN-γ) and IL-10 in the lung. IFN-γ-deficient CD4 cells produced larger amounts of IL-17 and similar levels of TNF-α, IL-10, and IL-2 compared to wild-type (WT) CD4 cells. Both WT and IFN-γ$^{-/-}$ CD4 cells exhibit influenza virus-specific cytotoxicity; however, IFN-γ-deficient CD4 cells did not promote recovery after lethal infection as effectively as WT CD4 cells. PR8 infection induced a population of cytolytic CD4 effectors that resided in the lung but not the DLN. These cells expressed granzyme B (GrB) and required perforin to lyse peptide-pulsed targets. Lethally infected mice given influenza virus-specific CD4 cells deficient in perforin showed greater weight loss and a slower time to recovery than mice given WT influenza virus-specific CD4 cells. Taken together, these data strengthen the concept that CD4 T cell effectors are broadly multifunctional with direct roles in promoting protection against lethal influenza virus infection.

Influenza virus infection remains a serious global health problem, with over 30,000 deaths each year in the United States. Immunocompromised individuals as well as the elderly and infants are at greater risk due to the lowered immune responses in these populations. In addition, the appearance of pandemic strains such as 2009 H1N1 underscores the need to develop new strategies to counteract this pathogen. Current vaccines against influenza virus rely on activating the humoral B cell response to induce high-affinity neutralizing antibodies against the outer coat proteins of the virus. However, these proteins undergo rapid mutation (antigenic drift) and can reassort in other animals such as swine (antigenic shift) to create new strains that have pandemic potential (38). While vaccine-induced neutralizing antibodies provide sterilizing immunity against the immunizing strain, vaccines must be reformulated each year to include the most prevalent circulating influenza viruses. In contrast to immunity against outer proteins, cellular immunity consisting of T cell responses is mainly directed against internal proteins of the virus, such as nucleoprotein (NP) and acid polymerase (PA). These internal proteins have a much lower mutation rate and tend to be conserved across many seasonal strains of influenza virus. Thus, it is important to understand the cellular immune response to influenza virus infection, to help in the design of more effective, universal influenza vaccines that protect against emerging pandemic and avian influenza virus strains.

Cellular immunity to influenza virus infection involves both CD8 and CD4 T cell subsets. It is widely believed that CD8 cells promote viral clearance via cytotoxic mechanisms, lysing virally infected epithelial cells. This direct mode of protection has been shown to utilize both perforin- and FasL-mediated cytotoxicity (41). In contrast, CD4 T cells are known to provide indirect help in viral clearance by secreting cytokines and inducing high-affinity antibodies that neutralize virus and provide protection against reinfection with the same strain (18, 23). CD4 T cells differentiate into T helper 1 (Th1) effectors in response to influenza virus infection and secrete large amounts of gamma interferon (IFN-γ) in the lung (31). IFN-γ expression is heterogeneous in T cells, and cells with the highest expression migrate to the lung (20). This cytokine is important for driving isotype switching to IgG2a and IgG3, as mice treated with anti-IFN-γ antibodies demonstrate lower anti-influenza virus titers (3). However, studies using mice deficient in IFN-γ suggest that this cytokine is dispensable for cytotoxic T lymphocyte (CTL) function and survival from lethal infection (15). Graham et al. also demonstrated that a CD4 T cell clone deficient in IFN-γ could protect mice from lethal influenza virus infection (15), and our own previous data confirmed that γ$^{-/-}$ CD4 effectors generated *in vitro* could protect from lethal challenge (7). However, the contribution of IFN-γ in the CD4 effector-mediated response to influenza virus infection and whether *in vivo*-generated CD4 effectors could promote protection by IFN-γ-mediated or cytolytic mechanisms were not addressed in these studies.

More recently, a direct role for CD4 T cells has been suggested in chronic infections, such as cytomegalovirus (CMV), Epstein-Barr virus, and HIV infections in humans (43) and gammaherpesvirus infections in mice (35). These data indicate that chronic

6792 jvi.asm.org
Journal of Virology p. 6792–6803
June 2012 Volume 86 Number 12

antigen exposure induces a highly differentiated CD4 T cell effector with cytolytic potential (1). These effectors express perforin and granzymes and undergo granule exocytosis upon antigen reexposure (9). Our previous work demonstrated that CD4 effectors generated *in vitro* could acquire cytolytic activity (7, 8) and were able to protect mice from a lethal dose of influenza virus using perforin-mediated cytolytic mechanisms in synergy with B cell help (7). However, it is not known whether CD4 cells activated during an acute infection can become cytotoxic or whether this activity helps control infection. In this study, we set out to determine the mechanisms used by CD4 T cells during an acute influenza viral infection, whether CD4 effectors generated *in vivo* could acquire cytolytic activity, and which mechanisms contributed to protection from a lethal dose of influenza virus. We found that CD4 cells have different effector profiles in the draining lymph node (DLN) than the lung and that CD4 cells secrete IFN-γ at the site of infection that can contribute to protection. In addition, CD4 cells acquire perforin-mediated cytotoxicity in the lung, but not the DLN, that may enhance recovery from lethal infection.

MATERIALS AND METHODS

Mice. BALB/c By mice were purchased from the Jackson Laboratory, Bar Harbor, ME. IFN-$\gamma^{-/-}$ mice on the BALB/c background (45) and BALB/c Thy1.1 mice, originally obtained from Jonathan Sprent (The Scripps Research Institute, La Jolla, CA) were maintained at the Trudeau Institute Animal Breeding Facility. T cell receptor (TCR) transgenic (Tg) mice in which CD4 cells recognize the hemagglutinin peptide from residues 126 to 138 (HA$_{126-138}$) from H1N1 influenza virus A/Puerto Rico 8/34 (PR8) were a gift from D. Lo (The Scripps Research Institute, La Jolla, CA) and have been described in detail (32). HA-specific TCR Tg mice, which we refer to as HNT mice (because the amino acid sequence of the peptide recognized by these cells begins with HNT), were bred to IFN-$\gamma^{-/-}$ and BALB/c Thy1.1 mice at the Trudeau Institute Animal Breeding Facility to generate HNT IFN-$\gamma^{-/-}$ mice and HNT Thy1.1 mice, respectively. Perforin-deficient (Pfn$^{-/-}$) mice on the BALB/c background were a gift from J. Harty (University of Iowa, Iowa City, IA) and were bred to HNT mice at the Trudeau Institute Animal Breeding Facility (7). B cell-deficient mice homozygous for a disruption at the JH locus (JHD) (30) backcrossed to BALB/c mice were also maintained at the Trudeau Institute Animal Breeding Facility. All experimental animal procedures were conducted in accordance with the Trudeau Institute Animal Care and Use Committee guidelines.

Influenza virus and infections. PR8 was grown in the allantoic cavity of embryonated hen's eggs as previously described (28). BALB/c or BALB/c IFN-$\gamma^{-/-}$ mice were infected intranasally with 500 egg infectious units (EIU) PR8 in 50 μl of phosphate-buffered saline (PBS) as a sublethal dose for analysis of CD4 effector functions or 5,000 to 10,000 EIU as a lethal dose for survival experiments.

Isolation of cell populations, adoptive transfer, and lethal infection. Influenza virus-infected BALB/c mice were sacrificed at various times postinfection (p.i.) with a lethal dose of tribromoethanol (Avertin) anesthesia intraperitoneally. Lungs were perfused via the right ventricle of the heart with PBS, minced, and incubated with collagenase D at a 2.5-mg/ml final concentration to dissociate lung tissue. Single-cell suspensions were filtered through 70-μm-mesh-size mesh and used in various assays or further incubated with anti-CD4-conjugated magnetic beads (clone GK1.5) according to the manufacturer's protocol (Miltenyi Biotec). We typically observed a >80% enrichment in CD4$^+$ T cell effectors from the lung, with each mouse yielding approximately 2×10^6 to 4×10^6 CD4 cells. DLN cells were dissociated, and single-cell suspensions were used in various assays or further enriched with anti-CD4 magnetic beads as described above. Total CD4 cells (1×10^7) were injected into naïve host mice and 18 h later infected with 5,000 to 10,000 EIU PR8 in 50 μl PBS intranasally (i.n.). Mice were then monitored for weight loss and survival over

the course of the experiment. Mice were euthanized when they became moribund, according to the Trudeau Institute Animal Care and Use Committee guidelines. Kaplan-Meier survival curves were generated, and statistical significance was analyzed by the log-rank test.

Isolation of TCR Tg CD4 cells and adoptive transfer. Naïve CD4 cells were isolated from TCR Tg mice using a positive-selection protocol with anti-CD4 beads (clone GK1.5) according to the manufacturer's protocol (Miltenyi Biotec, Cambridge, MA). Naïve HNT or HNT $\gamma^{-/-}$ CD4 cells (1×10^6 to 2×10^6) were injected via the tail vein into BALB/c and BALB/c IFN-$\gamma^{-/-}$ mice, respectively. In some experiments, wild-type (WT) HNT or HNT Pfn$^{-/-}$ CD4 cells were injected into naïve host mice via the tail vein. At 18 to 24 h after adoptive transfer, mice were infected i.n. with 500 EIU PR8. At 7 to 10 days postinfection, mice were sacrificed and CD4 cells were isolated from DLN and lung as described above. This population included TCR Tg CD4 cells as well as endogenous CD4 T cell effectors and was used for *in vitro* assays or survival studies where noted in the figure legends. Typically, 2 to 5% of the CD4 cells isolated from the DLN were HNT specific, while a range of from 6 to 12% of the CD4 cells in the lung were HNT specific.

Medium and peptides. All cells were grown in RPMI 1640 containing 2 mM L-glutamine, 100 IU penicillin, and 100 μg/ml streptomycin (all obtained from Invitrogen Life Technologies), 10 mM HEPES (Research Organics), 50 μM 2-mercaptoethanol (Sigma-Aldrich, St. Louis, MO), and 8% fetal bovine serum (FBS) (HyClone). HA peptide from residues 126 to 138 (HA$_{126-138}$; HNTNGVTAACSHE), HA peptide from residues 518 to 526 (HA$_{518-526}$; IYSTVAASL), NP peptide from residues 146 to 160 (NP$_{146-160}$; ATYQRTRALVRTGMD), and NP peptide from residues 216 to 230 (NP$_{216-230}$; RIAYERMCNILKGKF) were synthesized by New England Peptide (Gardner, MA).

Proliferation assay. DLNs were harvested from influenza virus-infected mice at 7 to 10 days postinfection, dissociated to a single-cell suspension, and incubated with irradiated $H-2^d$-expressing A20 B lymphoma cells as antigen-presenting cells (APCs) and specific influenza virus peptides at 37°C for 48 h. [^{3}H]thymidine (Amersham Biosciences, Piscataway, NJ) at 0.2 μCi/well was added for 18 h, plates were harvested using a Filtermate harvester (Perkin Elmer, Shelton, CT), and incorporated ^{3}H was measured using a Microbeta Trilux scintillation counter (Perkin Elmer). Results are expressed as a stimulation index, calculated by dividing the number of counts per minute obtained in wells stimulated with peptide or anti-CD3 by the number of counts per minute in medium control wells.

Enzyme-linked immunosorbent spot (ELISpot) assay for cytokine-secreting cells. Multiscreen HA plates (Millipore) were coated overnight with anti-IFN-γ antibody (clone R4-6A2; BD Biosciences) or anti-IL-17 antibody (R&D Systems, Minneapolis, MN) at 5 μg/ml in PBS. Plates were washed with PBS–Tween 20 and blocked using complete RPMI 1640 medium with 10% FBS. DLN or lung cells were added at 10^6 cells/well and serially diluted 1:2 in RPMI medium. Irradiated naïve splenocytes were added as APCs with or without major histocompatibility complex class II-restricted PR8 HA$_{126-138}$, HA$_{110-120}$, NP$_{147-160}$, and NP$_{216-230}$. Plates were incubated overnight at 37°C, washed with PBS–Tween 20, and incubated with biotinylated anti-IFN-γ antibody (clone XMG1.2; BD Biosciences) or biotinylated anti-IL-17 antibody (R&D Systems) at 1 μg/ml overnight at 4°C. Plates were washed with PBS–Tween 20 and incubated with streptavidin-alkaline phosphatase (ExtraAvidin; Sigma-Aldrich) at 1:500 for 1 h at 25°C. Spots were developed using a 1-mg/ml solution of 5-bromo-4-chloro-3-indolyl phosphate–nitroblue tetrazolium (BCIP/ NBT; Sigma-Aldrich). Spots were counted using an Immunospot counting system (Cellular Technologies, Ltd.). Data are plotted as the number of IFN-γ spots per input cell number.

Immunofluorescence. Frozen lung sections (5 μm) from PR8-infected and uninfected mice were blocked with PBS containing Fc Block (10 μg/ml) and 5% donkey serum (Jackson ImmunoResearch Laboratories, West Grove, PA) for 30 min at room temperature. To block endogenous biotin, lung sections were incubated with 100 μl of avidin (1 mg/ml) for 15 min at room temperature (RT), followed by 100 μl of biotin (1
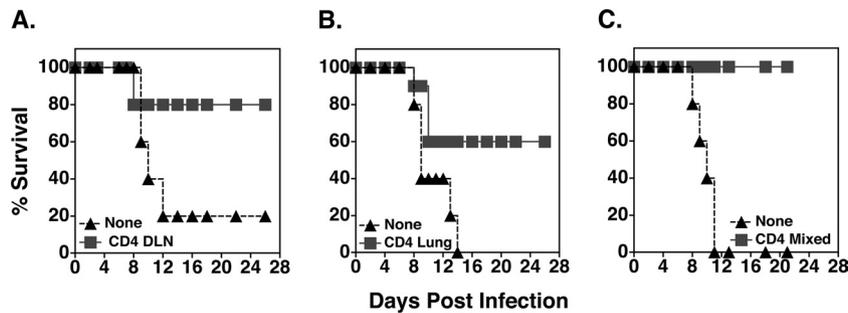
FIG 1 CD4 effectors from the DLN and lung provide protection from lethal-dose influenza virus infection. Healthy BALB/c mice were infected with 500 EIU PR8 i.n., and 7 to 10 days later, CD4 cells were isolated from the DLN or lung using anti-CD4-conjugated magnetic beads. CD4 cells from the DLN (A), lung (B), or DLN and lung combined (C) were adoptively transferred intravenously to naïve BALB/c mice that were subsequently infected with 5,000 EIU PR8, and survival was monitored over time. Kaplan-Meier curves were generated by Prism software. In all graphs, survival of mice given CD4 cells is significantly higher than that in mice left untreated (none) by the log-rank test ($P \leq 0.01$).

mg/ml) for 15 min at RT (Sigma). Lung sections were then incubated with biotin-conjugated anti-mouse I-A^d and fluorescein isothiocyanate (FITC) anti-mouse Thy1.1 (BD biosciences) for 30 min at RT. As a control, lung sections were incubated with an irrelevant isotype control (biotin-conjugated IGg2a,k; BD Biosciences). Class II was detected with streptavidin conjugated to Alexa Fluor 594 and T cells with anti-FITC conjugated to Alexa Fluor 488 (Molecular Probes, Carlsbad, CA). Type II alveolar epithelial cells were detected using rabbit polyclonal anti-prosurfactant protein C (Abcam, Cambridge, MA) (data not shown). Bound antibodies were detected with donkey anti-rabbit antibody conjugated to Texas Red (Jackson ImmunoResearch). Sections were mounted with medium for fluorescence with 4′,6-diamidino-2-phenylindole (Vector Laboratories, Burlingame, CA).

ICCS. CD4 T cells were isolated from DLN, spleen, or lung and restimulated for 4 h with 10 ng/ml phorbol myristate acetate (PMA) and 500 ng/ml ionomycin (Sigma-Aldrich) or for 6 h with peptide-pulsed A20 cells as APCs. Brefeldin A (10 μg/ml; Sigma-Aldrich) was added for the final 2 h of culture and maintained throughout the intracellular cytokine staining (ICCS) procedure. In some experiments, donor T cells were surface stained with anti-Thy1.1 or anti-Thy1.2 and anti-CD4 as described previously (7, 16), fixed in 100 μl 4% paraformaldehyde, and stained in saponin buffer (PBS plus 1% FBS, 0.1% NaN$_3$, and 0.25% saponin; Sigma-Aldrich) containing anti-IFN-γ–APC, anti-IL-17–phycoerythrin (PE), anti-IL-2–FITC or anti-tumor necrosis factor alpha (anti-TNF-α)–PE (all antibodies were purchased from BD Biosciences). In some experiments, APC-conjugated mouse anti-human granzyme B (GrB; clone GB12; Caltag, Burlingame, CA) was used to measure intracellular levels of GrB protein in infected samples. APC-conjugated mouse IgG1 was used as an isotype control (Caltag).

Reverse transcription-PCR for transcription factors and cytolytic markers. Mice were infected i.n. with 500 EIU PR8. Six to 8 days later, mice were sacrificed and CD4 cells were isolated from the lung and DLN by anti-CD4-conjugated magnetic beads. The flowthrough, enriched in CD8$^+$ cells, served as a positive control. Cells were resuspended in TRIzol and RNA extracted with a RiboPure kit from Ambion (Applied Biosystems, Carlsbad, CA). cDNA was reverse transcribed with a high-capacity cDNA reverse transcription kit (Applied Biosystems) according to the manufacturer's instructions and amplified using the following validated TaqMan primer/probe sets: for Eomesodermin (Eomes), Mm01351985; for T cell-specific transcription factor (T-bet), Mm00450960; for GrA, Mm00439191; for GrB, Mm00442834; and for Pfn, Mm 00812512 (Applied Biosystems). Mouse GAPDH (glyceraldehyde-3-phosphate dehydrogenase) was used as an endogenous control for amplification. Amplification was carried out using a Step-One Plus real-time PCR machine from Applied Biosystems, and relative quantity was calculated by the delta delta threshold cycle method using Applied Biosystems software.

JAM assay for cytotoxicity. Cytotoxicity was measured by the JAM (Just Another Method) assay (19) as described previously (8). CD4 cells

were isolated from DLN or lung as described above and plated at decreasing concentrations in 96-well round-bottom plates. A20 cells, labeled for 4 h with 4 μCi/ml [^{3}H]thymidine (Amersham Biosciences), were added to effectors at a concentration of 1×10^4 cells/well. HA$_{126-138}$ was added at a final concentration of 2 μg/ml. In some experiments, a mixture of HA and NP peptides was added at a concentration of 2 μg/ml. Labeled A20 cells without peptide served as a negative control. After 4 h at 37°C, plates were harvested and incorporated [^{3}H]thymidine was measured using a Microbeta Trilux scintillation counter (Perkin Elmer). In some experiments, anti-FasL (clone MFL3) was added at 5 to 10 μg/ml to inhibit Fas-mediated killing (8). Percent specific lysis was calculated as [(spontaneous counts per minute − experimental counts per minute)/spontaneous counts per minute] × 100 (19).

Statistical analyses. Statistical analyses were performed using Prism software. The log-rank test was used for survival curves, and Student's two-tailed unpaired t test was used for analysis of statistical significance between experimental samples.

RESULTS

CD4 effectors from the DLN and lung provide protection from lethal influenza virus infection. Our previous results have demonstrated that Th1-polarized, *in vitro*-generated CD4 T cell effectors provide protection against a lethal dose of highly pathogenic H1N1 virus, PR8 (7). We next wanted to determine if CD4 cells generated *in vivo* in response to sublethal PR8 infection could confer protection to naïve mice given a lethal challenge. Figure 1A demonstrates that total CD4 cells isolated from the DLNs of healthy BALB/c mice 7 days after sublethal infection could confer protection against a lethal dose of PR8 when transferred to naïve BALB/c mice. Similarly, CD4 cells isolated from the lung could also confer protection against lethal challenge, but typically, not all mice were protected from lethal challenge (Fig. 1B). Protection was also observed when CD4 cells were isolated from the DLN and lung and mixed prior to transfer and subsequent lethal infection (Fig. 1C). Thus, terminally differentiated CD4 effectors in the lung and activated CD4 cells in the DLN contribute to protection mediated by CD4 helper T cells.

CD4 cells display different functional properties in the DLN than the lung. We next wanted to investigate the level of activation and possible effector functions used by CD4 T cells that may be responsible for protection. To investigate this, we first analyzed the polyclonal response against endogenous influenza virus CD4 epitopes using BALB/c mice infected with 500 EIU PR8 and sacrificed at various times postinfection (Fig. 2A). Cell suspensions from the DLN and lung were assayed for the ability
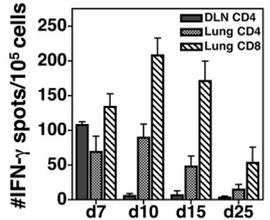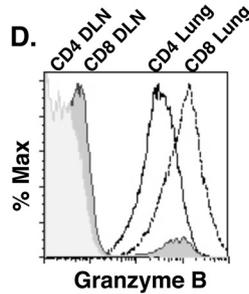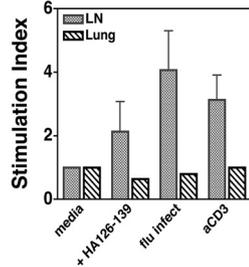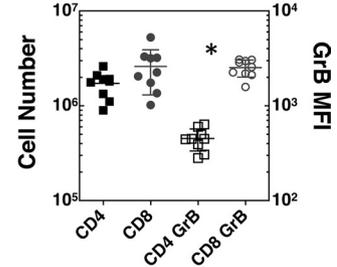
A. endogenous response

500 EIU PR8

BALB/c

7 10 15 25

Analysis of CD4 and CD8
functional responses

B.

- DLN CD4
- Lung CD4
- Lung CD8

#IFN-γ spots/10^5 cells

d7 d10 d15 d25

C.

- LN
- Lung

Stimulation Index

media + HA126-139 flu infect aCD3

D.

% Max

CD4 DLN CD8 DLN CD4 Lung CD8 Lung

Granzyme B

E.

Cell Number

GrB MFI

CD4 CD8 CD4 GrB CD8 GrB

F. endogenous + TCR tg response

WT HNT/Thy1.1 cells

500 EIU PR8

BALB/c

4 7 11

Analysis of CD4 functional
responses from DLN, lung,
spleen by gating on CD4/
Thy1.1+ cells

G.

CD4

DLN 2.32   Spleen 0.3   Lung 11.1

Thy 1.1

H.

% CD4/Thy1.1+

- DLN
- Lung
- Spl

Time (days)

I. ex vivo

% Max

- Lung
- Spl
- DLN

GrB

J. peptide restimulation

% Max

- Lung
- Spl
- DLN

IL-2   IFN-γ

K.

% cytokine (+)

GrB MFI

- IFN-γ
- IL-2
- IL-10
- GrB

DLN Lung Spleen
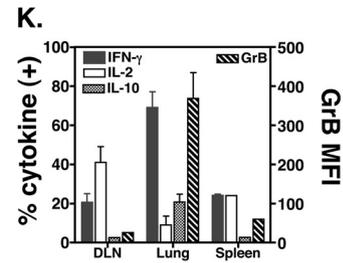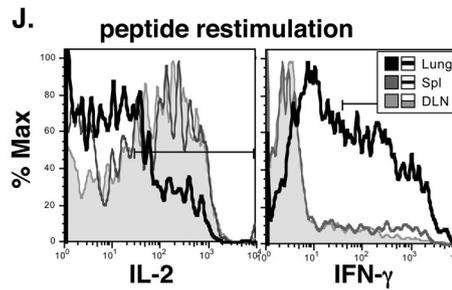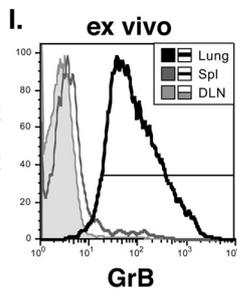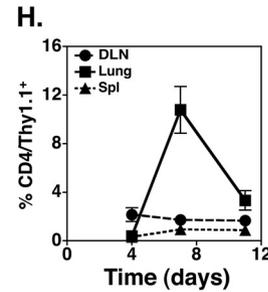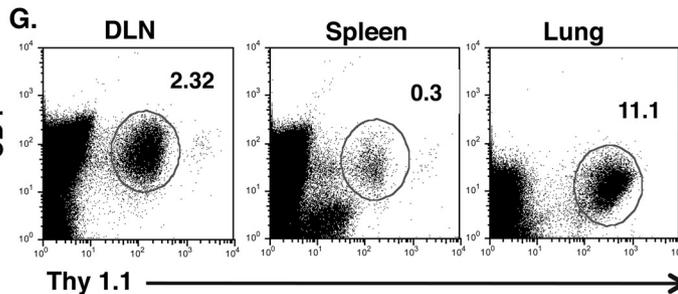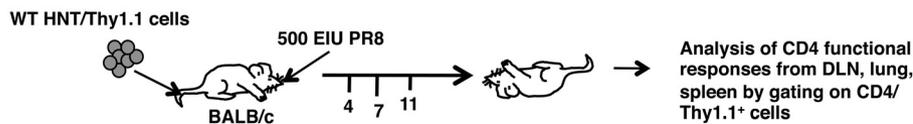
FIG 2 CD4 cells display different functional properties in the DLN than the lung. (A) BALB/c mice were infected with 500 EIU, and DLN and lung cells were isolated at various times postinfection to analyze the endogenous response. (B) Number of cells secreting IFN-γ per 1×10^5 total input cells incubated with class II-restricted peptides $HA_{126-138}$ and $NP_{216-230}$. Cells were also incubated with the class I-restricted $NP_{147-160}$ as a positive control. (C) At day 7 postinfection, DLN and lung cells were isolated and incubated with $HA_{126-138}$-pulsed A20 cells, influenza virus-infected A20 cells, or anti-CD3 for 3 days, with [^{3}H]thymidine added for the last 18 h. Shown is the average fold expansion over that for the medium control for three separate experiments. (D) DLN and lung cell preparations isolated at day 8 were incubated with antibodies to CD4, CD8, and GrB and subjected to flow cytometric analysis. A representative histogram of GrB expression gated on CD4 or CD8 cell populations is shown. (E) Total CD4 or CD8 T cell numbers (left axis) in the lungs of influenza virus-infected mice were calculated by multiplying total cell numbers by percent CD4- or CD8-positive cells analyzed by flow cytometry and the mean fluorescence intensity (MFI; right axis) of GrB expression in individual mice. *, $P = 0.0001$ by unpaired Student's t test. (F) HNT Thy1.1 CD4 cells (1×10^6 to 2×10^6) were adoptively transferred into healthy BALB/c mice, and the mice were subsequently infected with 500 EIU PR8. At 7 days postinfection, DLN, spleen, and lung cell populations were isolated as described in Materials and Methods and incubated with antibodies to CD4 and Thy1.1 to identify HNT peptide-specific CD4 cells. (G) Percentage of HNT cells in each organ at day 7 p.i. from a representative experiment. (H) Average percentage ± SD of CD4 Thy1.1 cells over time. (I) CD4 Thy1.1+ cells gated in panel G were analyzed for expression of GrB directly *ex vivo*. The gate depicts cells that are positive for expression based on the isotype control. (J) DLN, spleen, and lung cells isolated as in panel F were further restimulated with $HA_{126-138}$ for 4 h *in vitro* and analyzed for the ability to produce IL-2 and IFN-γ by flow cytometry. Histograms show cells that were gated on CD4 and Thy1.1, as in panel G. The gate depicts cells that are positive for cytokine expression based on staining in the medium controls. Samples were run on a BD FACScaliber apparatus, and data were analyzed using Flow Jo software. (K) Average percentage ± SD of cytokine-secreting cells (left axis) or GrB MFI (right axis) of CD4/Thy1.1+ cells in various organs at 7 days postinfection in three separate experiments.

to secrete cytokines (Fig. 2B) and proliferate (Fig. 2C) upon peptide restimulation. To determine the extent of cytokine secretion, DLN and lung single-cell suspensions were incubated with a mixture of CD4-specific HA and NP peptides or the class I binding CD8-specific $NP_{147-159}$ as a positive control. CD4 IFN-γ responses in the DLN peak early, at day 7, and decline thereafter, while the frequency of CD4 cells able to secrete IFN-γ in the lung peaks at day 10. The frequency of CD8 cells responding to NP peptide is approximately 2- to 3-fold higher than the frequency of CD4 cells responding to HA and NP peptides at all time points tested, with CD8 cells also peaking at day 10 postinfection. This indicates that CD4 T cells produce a substantial Th1-type response but that the response is lower in magnitude than the CD8 T cell response, similar to our previous work using TCR Tg CD4 and CD8 populations (28). At 7 days postinfection, DLN cells proliferated in response to restimulation, while cells from the lung did not divide. CD4 cells proliferated in response to $HA_{126-138}$ 2-fold over medium controls, and the response to influenza virus-infected APCs was higher at approximately 4-fold (Fig. 2C).

Our previously published data showed that Th1-polarized, *in vitro*-generated CD4 effectors expressed the serine protease GrB and acquired perforin-mediated cytolytic activity (7, 8). To determine if CD4 T cell effectors generated *in vivo* also had this activity, DLN and lung cells were stained with anti-CD4, anti-CD8, and anti-GrB antibodies. Figure 2D demonstrates that CD4 cells residing in the lung 8 days after influenza virus infection express GrB, but only approximately 0.4% of the cells in the DLN express this protein. A higher proportion of CD8 T cells in the DLN ($\approx$6%) express GrB, and all of the CD8 cells in the lung express GrB at high levels. Indeed, the mean fluorescence intensity (MFI) of GrB expression in CD8 cells is 5-fold higher than the MFI of GrB expression in CD4 cells (Fig. 2E). Thus, CD4 T cells can proliferate and secrete IFN-γ upon restimulation and express high levels of GrB directly *ex vivo* after influenza virus infection. Although CD8 T cell responses are higher in magnitude in the lung, expression of GrB by CD4 cells suggests that they may have a direct role in viral clearance and protection.

To further analyze the CD4 response to influenza virus infection, we employed a TCR Tg mouse model in which all CD4 cells recognize the $HA_{126-138}$ in the context of class II I-A^d, termed HNT mice. Approximately 1×10^6 HNT CD4 cells were adoptively transferred into healthy BALB/c mice that were then infected with a sublethal dose of PR8 (Fig. 2F). At 4, 7, and 11 days postinfection, single-cell suspensions from various organs were isolated and the percentage of CD4 Thy1.1 cells was analyzed by flow cytometry. Figure 2G shows representative histograms of HNT-specific cells, with frequencies of 2.3% in the DLN, 0.3% in the spleen, and 11.1% in the lung at day 7 p.i. The average percentage of HNT-specific cells in the DLN, lung, and spleen over time is shown in Fig. 2H, and the results confirm that peak CD4 T cell responses in the adoptive transfer model occur at approximately day 7 (28, 31). Gating on CD4 Thy1.1-positive (Thy1.1$^+$) or $HA_{126-138}$-specific cells demonstrates that cells isolated from the lung are more activated, indicated by high levels of the activation isoform of CD43 (data not shown) and expression of GrB (Fig. 2I). In contrast, HNT-specific cells from the DLN and spleen do not express GrB. To analyze cytokine secretion, CD4 cells were isolated at day 7 postinfection and assayed for the ability to produce IL-2 or IFN-γ in response to $HA_{126-138}$. Figure 2J shows
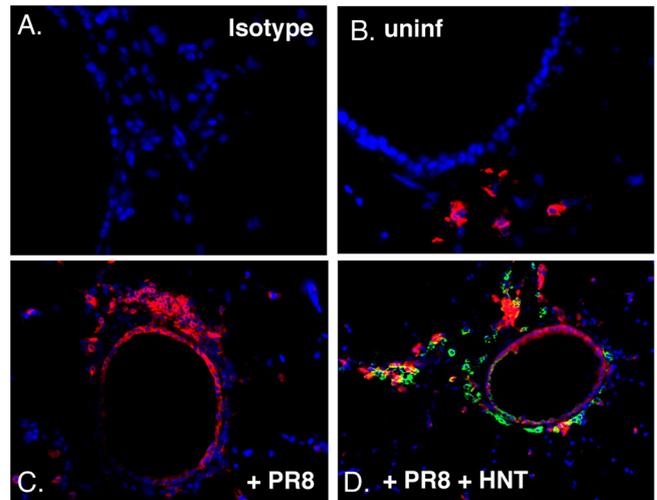

FIG 3 Lethal influenza virus infection induces class II expression on lung epithelial cells. Mice were given HNT Thy1.1$^+$ effectors and subsequently infected with 5,000 EIU PR8. Five days later, mice were sacrificed and lungs were frozen as described in Materials and Methods. Shown is immunofluorescent analysis of frozen lung sections from uninfected mice (B), mice infected with 5,000 EIU PR8 (A and C), or infected mice given HNT Thy1.1$^+$ CD4 cells (D) incubated with antibodies against class II (red) or Thy1.1 (green). (D) Staining of HNT-specific CD4 cells (green) in proximity to epithelial cells expressing class II (red). Magnification, $\times$200.

representative histograms, while Fig. 2K quantifies the percentage of positive cytokine-expressing cells in each organ. Restimulation of the CD4$^+$ fractions with HNT mouse peptide and subsequent gating on CD4 Thy1.1 populations demonstrate that almost half of all influenza virus-specific cells express IL-2 in the lymphoid organs but only about 20% of cells express IFN-γ. Conversely, almost 80% of HNT-positive cells in the lung express IFN-γ, but only about 10% of cells express IL-2 (Fig. 2J and K). In addition, high expression of GrB *ex vivo* correlates with IFN-γ expression after restimulation (Fig. 2K, left and right axes). Thus, in the infected site, Th1-polarized CD4 T cells develop, as do effectors that express high levels of GrB. In contrast, cells expressing high levels of GrB and IFN-γ are rare in the DLN.

Lethal influenza virus infection induces class II expression on epithelial cells, providing targets for cytolytic CD4 cells residing in the lungs. Because CD4 T cells could differentiate to effector cells with cytolytic activity, we wanted to determine whether the infected lung could provide potential class II-expressing targets for killing. In this experiment, we adoptively transferred *in vitro*-generated CD4 effectors that acquired perforin-mediated cytolytic activity (7) and analyzed class II expression in the lung 5 days after lethal infection. Figure 3B shows that epithelial cells in uninfected lungs do not express class II and class II staining is restricted to cells in the parenchyma, probably macrophages. In contrast, lethal infection induces the expression of class II on epithelial cells in the airways (Fig. 3C). This correlates with cytokeratin expression in the same cells (data not shown). Importantly, *in vitro*-generated CD4 T cell effectors can be seen in close proximity to the airways in the peribronchial areas of the lung (Fig. 3D). Since *in vitro*-generated cytolytic CD4 cells protect mice against lethal influenza virus infection in a perforin-dependent manner and lethal infection upregulates class II on epithelial cells, we next set out to determine whether CD4 T cells generated during sublethal influenza virus infection were cytolytic *in vivo*.
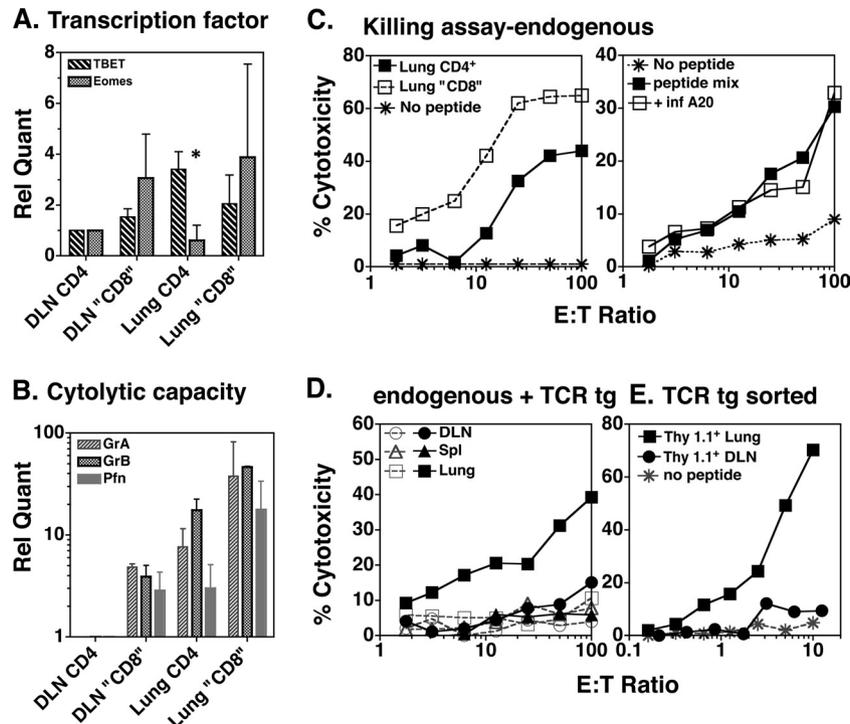
FIG 4 Lung resident CD4 cells express granzymes and perforin and lyse peptide-pulsed targets. (A and B) Mice were infected with 500 EIU, and at 8 days postinfection, CD4 cells were isolated from the DLN or lung as described in the text. The non-CD4 cells were used as a control that contained CD8 T cells. Shown is the relative quantity of T-bet and Eomes (A) or GrA, GrB, and perforin (B) mRNA by real-time PCR using CD4 cells from the DLN as the reference sample. Lung CD4 cells express significantly higher levels of T-bet than Eomes ($P = 0.006$ by Student's unpaired t test). Shown is an average from three separate cell isolations. (C) Mice were infected and cells were isolated as described for panels A and B and assayed for cytotoxicity against A20 cells pulsed with influenza virus-specific class I peptides ($NP_{147-156}$ and $HA_{518-526}$) or class II peptides ($HA_{126-138}$, $NP_{216-230}$, and $NP_{146-160}$) (left) or A20 cells pulsed with class II peptides or infected with influenza virus (right). This experiment was repeated, with similar results. HNT Thy1.1 cells (1×10^6) were adoptively transferred to BALB/c mice that were then infected with 500 EIU PR8. E:T, effector-to-target cell ratio. (D and E) Total CD4 cells were isolated by magnetic beads which contain endogenous and TCR Tg CD4 cells (D) or $Thy1.1^+$ cells, isolated by FACS, which are purified TCR Tg cells (E), from the DLN, spleen (Spl), and lung and incubated with HNT-pulsed A20 target cells in a 4-h cytotoxicity assay. Shown is the percent lysis of each population against peptide-pulsed (closed symbols) or unpulsed (open symbols) target cells. These experiments were repeated once (E) or twice (D) with similar results.

We first analyzed the cytolytic capacity of CD4 cells in the lung by evaluating the expression of mRNA for proteins known to be important for CD8 CTL differentiation (26, 27). Because CD4 cells in the DLN did not express GrB protein (Fig. 2D), these cells were used as a reference sample in the quantitative PCR assays, while CD8-enriched populations were used as positive controls. Figure 4A demonstrates that CD4 cells isolated from the lung 8 days after sublethal infection upregulate the canonical Th1 transcription factor, T-bet. However, the level of Eomes expression is lower in lung resident CD4 cells but higher in lung resident CD8 cells than the levels expressed in CD4 cells in the DLN. CD4 cells in the lung show significantly higher expression of T-bet mRNA than Eomes mRNA, suggesting that protein levels may also be different. Figure 4B also indicates that lung resident CD4 cells show transcriptional upregulation of GrA, GrB, and Pfn compared to CD4 cells isolated from the DLN. CD4 cells express less Pfn and GrB mRNA than CD8 cells, and this correlates with the expression of GrB protein observed in Fig. 2E. Thus, CD4 cells residing in the lung have acquired the capacity to kill, as measured by upregulation of mRNA for proteins contained in cytolytic granules. We next wanted to determine if CD4 cells could lyse class II-restricted peptide-coated targets and analyzed both the endogenous polyclonal response (Fig. 4C) and the HNT-specific response after transfer of TCR Tg CD4 cells (Fig. 4D and E). Figure

4C demonstrates that CD4 cells isolated from the lung can lyse A20 targets pulsed with a mixture of $HA_{126-138}$ and $NP_{216-230}$, although less effectively than CD8 cells against targets pulsed with $HA_{518-526}$ and $NP_{147-160}$. In a separate experiment, total CD4 cells isolated from the lung lysed peptide-pulsed as well as A20 targets infected with PR8. Although cytolytic activity could be measured in the polyclonal endogenous population of CD4 cells, we reasoned that killing activity in HNT-specific CD4 cells would be easier to detect and used the same adoptive transfer method outlined in Fig. 2F to analyze CTL activity in HNT-specific cells. Isolation of total CD4 cells from the DLN, spleen, and lung at 7 days after influenza virus infection demonstrates that CD4 cells in the lung lyse HNT peptide-coated targets, while CD4 cells from the DLN and spleen lack this activity (Fig. 4D). In this experiment, the frequency of HNT-specific cells in the DLN was approximately 3%, while the frequency of HNT cells in the lung was closer to 12%. Thus, there could be cytolytic activity in the DLN, but since the frequency of cells is low, we may not be able to detect this activity in the CTL assay. To circumvent this problem, $Thy1.1^+$ HNT-specific CD4 cells were sorted from either DLN or lung by fluorescence-activated cell sorting (FACS) and used at the same cell number in the CTL assay. Figure 4E confirms that cells in the lung are highly cytolytic but cells in the DLN lack this activity. Taken together, these data indicate that CD4 effectors have cyto-
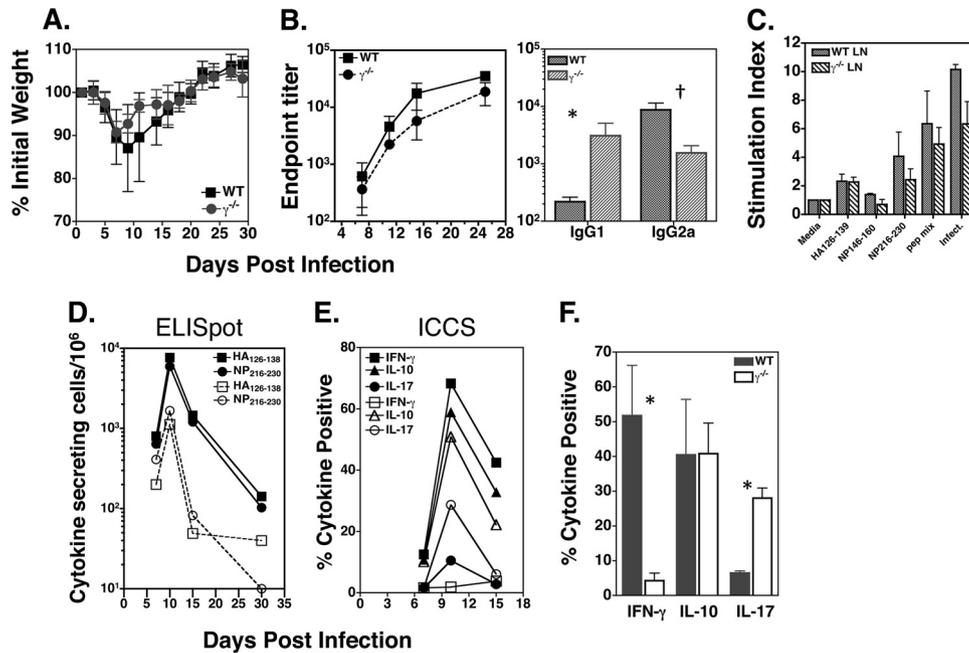
FIG 5 IFN-γ is not required for the multifunctional CD4 T cell response to influenza virus infection. (A) BALB/c (WT) or BALB/c mice deficient in IFN-γ ($\gamma^{-/-}$) were infected with 500 EIU and their weights were monitored over time. (B) Mice were bled at the indicated time points and analyzed for total influenza virus-specific IgG (left) or influenza virus-specific IgG1 or IgG2a (right) at day 25 p.i. by enzyme-linked immunosorbent assay. Shown is the endpoint titer. *P* values were determined by Student's *t* test: *, $P = 0.028$; †, $P = 0.002$. (C) Cells from the DLN of WT and IFN-$\gamma^{-/-}$ mice were restimulated *in vitro* with various influenza virus-specific peptides for 72 h, and [³H]thymidine incorporation was measured as an indication of proliferation. Shown is the stimulation index calculated as the fold increase over cells incubated in medium alone of three separate experiments. (D) CD4 cells were isolated from the lungs of WT (closed symbols) or IFN-$\gamma^{-/-}$ (open symbols) influenza virus-infected mice at various time points and incubated with HA or NP peptides in an ELISpot assay for IFN-γ (closed symbols) or IL-17 (open symbols). Shown is the number of cytokine-secreting spots calculated for 1×10^6 CD4$^+$ cells. (E) CD4 cells were isolated from the lungs of WT (closed symbols) or IFN-$\gamma^{-/-}$ (open symbols) influenza virus-infected mice at various time points and incubated with PMA and ionomycin. The percentage of cytokine-positive cells after gating on activated (CD4$^+$/CD43$^+$) cells is shown over time for one representative experiment. (F) Shown is the average ± SD of percent cytokine-positive cells in WT and IFN-$\gamma^{-/-}$ CD4 cells restimulated with PMA and ionomycin at day 10 p.i. from three separate experiments. *, statistically significant difference in percent cytokine-positive cells between WT and IFN-$\gamma^{-/-}$ cells ($P < 0.005$).

lytic activity in the lung but not in the DLN. Furthermore, influenza virus infection induces class II expression on epithelial cells that can potentially serve as a target for cytolytic CD4 cells in the lung.

IFN-γ is not required for the multifunctional CD4 T cell response to influenza virus infection. Because the anti-influenza virus CD4 response is predominantly Th1 mediated, with high levels of IFN-γ being secreted at the site of infection, we wanted to determine the role of this cytokine during the generation of CD4 effectors. First, we wanted to examine whether an absence of IFN-γ had any effect on morbidity, as measured by weight loss after sublethal infection. Figure 5A demonstrates that BALB/c WT or IFN-$\gamma^{-/-}$ mice display similar weight loss curves, suggesting that the course of infection is similar between the two groups of mice. Second, we also wanted to determine whether the helper function of CD4 cells was intact in these mice and looked at anti-influenza virus total IgG antibody titers as well as the titers of the IgG1 and IgG2a subtypes. Figure 5B shows that anti-influenza virus antibody titers are similar between WT and IFN-$\gamma^{-/-}$ mice over time but that WT mice produce significantly higher levels of anti-influenza virus IgG2a, while IFN-$\gamma^{-/-}$ mice express more anti-influenza virus IgG1. In addition, the proliferative responses of CD4 T cells in the DLN were comparable between WT and IFN-$\gamma^{-/-}$ mice (Fig. 5C), suggesting that the frequency of CD4 cells responding to influenza virus is similar between WT and IFN-$\gamma^{-/-}$ mice. We then isolated CD4 cells from the lungs of both

WT and IFN-$\gamma^{-/-}$ mice and investigated the ability of these cells to secrete cytokines by ELISpot assay (Fig. 5D) and ICCS (Fig. 5E). We measured the ability of IFN-$\gamma^{-/-}$ cells to produce IL-17 since CD4 cells have been shown to produce IL-17 in the absence of IFN-γ (11, 13). CD4 cells from WT mice produce IFN-γ in response to HA and NP peptides with a frequency of approximately 1 in 100 at the peak of the response for the dominant HA and NP peptides (Fig. 5D, closed symbols). IFN-$\gamma^{-/-}$ CD4 cells produce IL-17 in response to specific peptides, although the response to the dominant HA and NP peptides is approximately 10-fold lower (Fig. 5D, open symbols). CD4 responses in both WT and IFN-$\gamma^{-/-}$ mice peak at day 10 postinfection. In addition, cytokine responses to PMA and ionomycin show that over half of WT CD4 cells in the lung can produce IFN-γ and/or IL-10 (Fig. 5E and F, closed symbols). Similar frequencies of lung CD4 cells from IFN-$\gamma^{-/-}$ mice produce IL-10, but only about 30% of cells produce IL-17 (Fig, 5E and F, open symbols). CD4 cells from WT and IFN-$\gamma^{-/-}$ mice produce TNF-α and IL-2 in response to sublethal influenza virus infection at about the same frequency (data not shown). In addition, data obtained using multiplex cytokine assays reveal that CD4 cells from IFN-$\gamma^{-/-}$ mice produce more Th2-type cytokines than WT in response to influenza virus infection (data not shown). Therefore, CD4 effector functions are not severely impacted in the absence of IFN-γ, and CD4 cells deficient in IFN-γ produce more IL-17, perhaps as a compensatory mechanism.
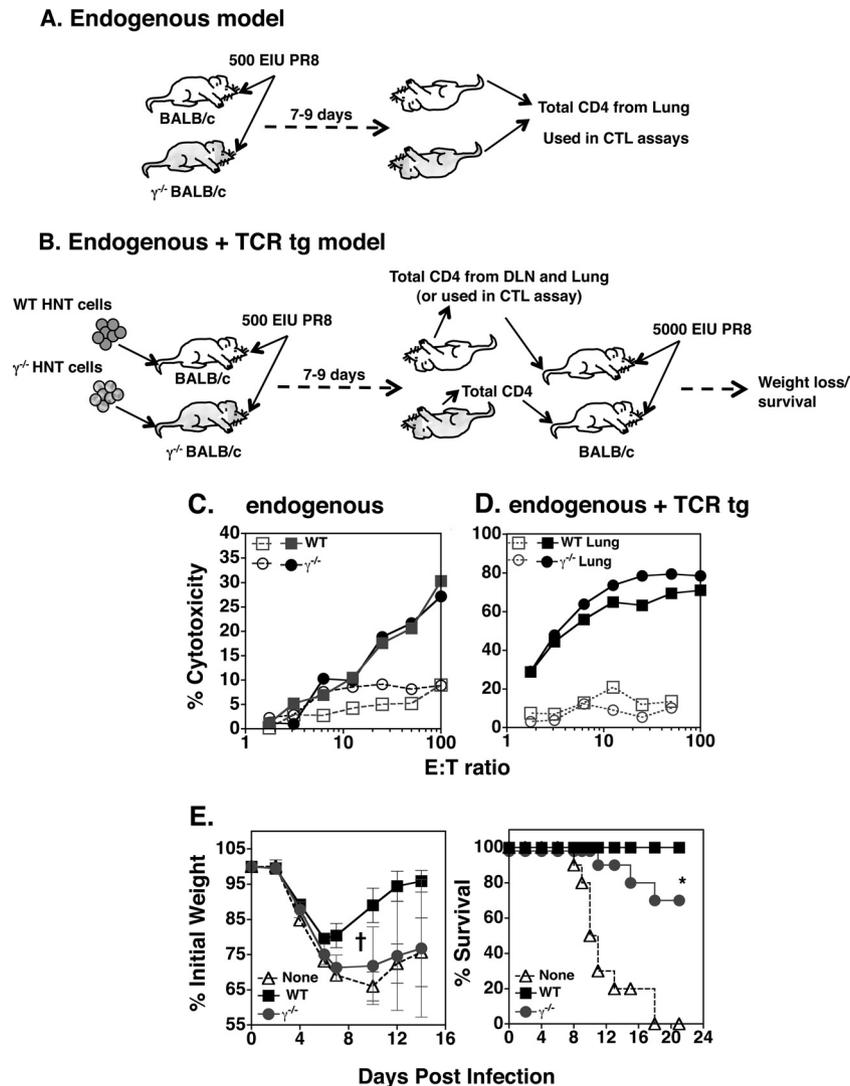
FIG 6 IFN-γ is dispensable for CTL activity but is necessary for complete protection from weight loss. (A) Schematic of endogenous CD4 effector generation for analysis of CTL activity. WT or IFN-γ$^{-/-}$ mice were infected with 500 EIU, and at day 9, mice were sacrificed and total CD4 cells were isolated for CTL assays (C). (B) Schematic of endogenous plus TCR Tg CD4 effector generation and transfer for CTL analysis (D) and protection studies. WT or IFN-γ$^{-/-}$ HNT cells are first transferred to WT or IFN-γ$^{-/-}$ mice before infection with 500 EIU. Total CD4 cells are then isolated as described at day 7 and used in CTL assays (D) or protection studies (E). (C) Total CD4 cells from the lung were isolated as described and assayed for cytotoxicity against A20 target cells pulsed with a mixture of class II peptides (closed symbols). Unpulsed A20 cells (open symbols) served as controls for antigen-specific killing. (D and E) Total CD4 cells were isolated from the lungs of mice receiving TCR Tg cells and assayed for cytotoxicity against HNT-pulsed A20 target cells (D) or transferred to healthy BALB/c mice that were then infected with 5,000 EIU PR8 and monitored for weight loss and survival (E). Shown is percent initial weight (left) and survival (right) over time from 10 individual mice. †, statistically significant difference in percent initial weight at day 9 ($P = 0.002$) by Student's t test; *, $P = 0.06$ by log-rank test.

IFN-γ is dispensable for CTL activity but is necessary for complete protection from weight loss. We next asked whether lack of IFN-γ had any effect on generation of cytolytic activity by CD4 T cells. We again analyzed the polyclonal response in WT and IFN-γ$^{-/-}$ mice infected with 500 EIU PR8 (Fig. 6A) and the TCR Tg response of HNT and HNT IFN-γ$^{-/-}$ CD4 cells adoptively transferred to WT and IFN-γ$^{-/-}$ mice, respectively (Fig. 6B). Lung resident CD4 cells isolated from WT or IFN-γ$^{-/-}$ mice at day 7 to 9 after influenza virus infection express similar levels of GrB (data not shown) and can lyse targets expressing a mixture of HA and NP peptides (Fig. 6C, closed symbols). Similarly, total CD4 cells isolated from the lungs of WT mice with HNT cells and IFN-γ$^{-/-}$ mice with HNT IFN-γ$^{-/-}$ cells can lyse HA$_{126-138}$-

coated targets with high activity (Fig. 6D, closed symbols). Importantly, WT and IFN-γ$^{-/-}$ CD4 cells possess the same level of cytolytic activity and possess approximately the same frequency of CD4 cells reactive to influenza virus peptides.

Because WT and IFN-γ$^{-/-}$ CD4 cells possessed the same relative functional abilities, that is, promotion of antibody class switching, ability to secrete cytokines, and lysis of target cells, we hypothesized that WT and IFN-γ$^{-/-}$ CD4 cells would be equally able to promote survival in a lethal challenge experiment, similar to our findings obtained using *in vitro*-generated effectors (7). To increase the number of influenza virus-specific CD4 cells in this system, we used the endogenous plus TCR Tg model outlined in Fig. 6B. Figure 6E (left) demonstrates that mice given IFN-γ$^{-/-}$ CD4 cells lose significantly
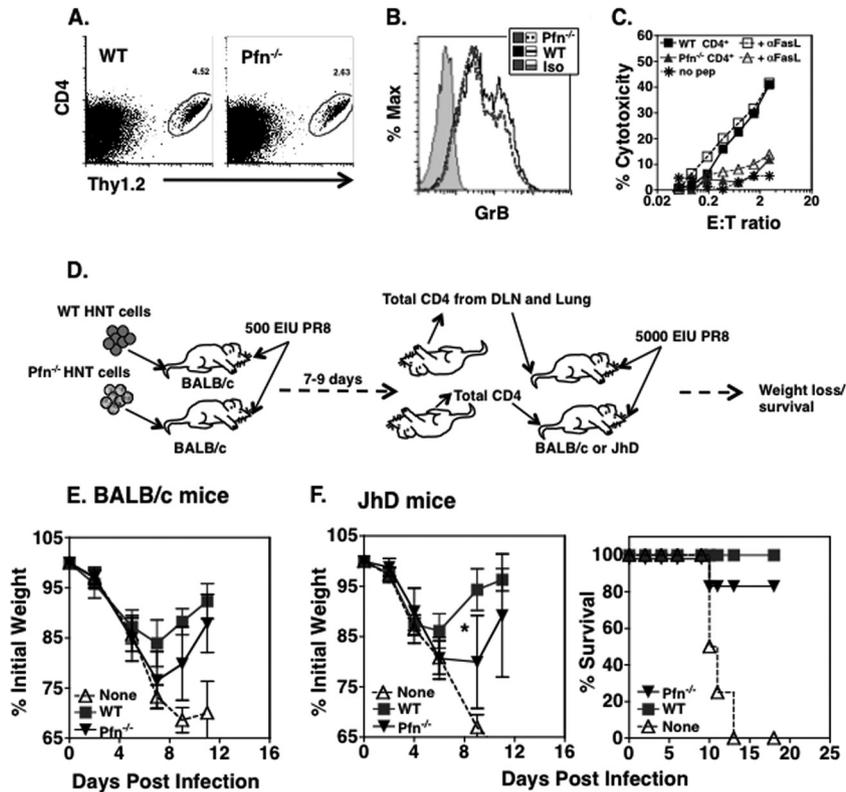
FIG 7 Perforin is required for cytolytic activity by CD4 T cells *in vivo* and may be important for faster recovery from lethal influenza virus infection. (A) WT or Pfn$^{-/-}$ HNT cells were adoptively transferred to BALB/c Thy1.1 mice that were then infected with 500 EIU PR8. Total lung cells were isolated and incubated with antibodies to CD4 and Thy1.2 to detect adoptively transferred HNT cells. (B) Relative level of GrB expressed by CD4$^+$ Thy1.2$^+$ WT or Pfn$^{-/-}$ HNT cells after gating on the cells shown in panel A. (C) Total CD4 cells were isolated from the lung using anti-CD4-conjugated magnetic beads and assayed for cytotoxicity against HNT peptide-pulsed targets. Closed symbols denote effectors incubated with HNT peptide-pulsed targets, and open symbols denote effectors incubated with HNT peptide-pulsed targets in the presence of antibodies to FasL. (D) Schematic of transfer protocol for weight loss and survival studies. WT or Pfn$^{-/-}$ HNT cells were adoptively transferred to BALB/c mice that were then infected with 500 EIU PR8. At 7 days p.i., total CD4 cells were isolated from the lung and DLN and transferred to healthy BALB/c or JhD mice that were then infected with 5,000 EIU PR8 and monitored for weight loss and survival. (E) Percent initial weight over time for 10 BALB/c mice per group. (F) Total CD4 cells were isolated as described and transferred to JhD mice deficient in B cells. Percent initial weight (left) and survival (right) over time are shown for 10 mice per group. *, a statistically significant difference in percent initial weight at day 9 ($P = 0.002$) by Student's *t* test.

more weight and are slower to recover than mice given WT CD4 cells. Mice given IFN-$\gamma^{-/-}$ CD4 cells appear to exhibit greater mortality than mice given WT CD4 cells; however, this does not reach significance ($P = 0.06$). Taken together, these data indicate that IFN-γ may have a role in generation of, or protection mediated by, *in vivo*-generated effectors that was not apparent in our studies using *in vitro*-generated effectors (7).

Perforin is required for cytolytic activity by CD4 T cells *in vivo* and may be important for faster recovery from lethal influenza virus infection. CD4 cells demonstrate a variety of functional responses as a consequence of influenza virus infection. It is becoming clear that CD4 T cells can contribute to antiviral responses using B cell- or helper-dependent mechanisms as well as B cell-independent or direct mechanisms (7, 14, 39, 40). Since CD4 cells could express GrB and acquired cytolytic activity, we wanted to determine whether this function was perforin mediated and whether perforin could contribute to protection mediated by CD4 cells. To this end, HNT-specific CD4 T cell Tg mice were crossed to perforin-deficient (Pfn$^{-/-}$) mice to obtain influenza virus-specific CD4 T cells that cannot express perforin. WT or Pfn$^{-/-}$ HNT cells were adoptively transferred to healthy BALB/c mice that were then infected with 500 EIU PR8. Figure 7 demonstrates that sim-ilar percentages of WT and Pfn$^{-/-}$ cells migrate to the lung (Fig. 7A) and express comparable levels of GrB (Fig. 7B). Total CD4 cells were then isolated from the lung and assayed for the ability to lyse HNT peptide-pulsed target cells. Figure 7C demonstrates that WT HNT cells lyse HNT peptide-coated targets, while Pfn$^{-/-}$ HNT cells do not. Furthermore, cytolytic activity in WT HNT cells is not inhibited by antibody to FasL, suggesting that the main mechanism of killing by adoptively transferred WT HNT cells is perforin mediated.

To determine whether perforin contributes to protection mediated by CD4 T cells, WT or Pfn$^{-/-}$ HNT cells were transferred to healthy BALB/c mice that were then infected with 500 PR8. At 7 days postinfection, total CD4 cells were isolated from the DLN and lung and transferred to BALB/c (D) or JhD (E) mice that were then infected with a lethal dose of PR8 (depicted in Fig. 7D). As seen in Fig. 7E, BALB/c mice given Pfn$^{-/-}$ CD4 cells lose slightly more weight than mice to which WT CD4 cells are adoptively transferred, although this did not reach significance. We reasoned that a clear difference in weight loss and survival may be difficult to discern due to the fact that CD4 effectors can also provide help for B cell responses, as we have shown previously (7, 18). Therefore, we repeated these experiments in JhD B cell-deficient mice

on the BALB/c background. In the absence of B cells, at day 9 postinfection, the percent initial weight in JhD mice to which $Pfn^{-/-}$ cells were transferred is statistically lower than that in JhD mice to which WT cells were transferred. Additionally, mice given WT CD4 cells recover faster and have a slightly higher survival rate than mice given $Pfn^{-/-}$ CD4 cells, although this increased survival does not reach statistical significance. These data support the concept that perforin-mediated cytotoxicity may play a role in protection conferred by CD4 T cells, but other CD4 effector functions such as cytokine secretion and B cell help may obscure the contribution of cytolytic activity. Taken together, our results indicate that CD4 effectors are multifunctional, with distinct activities in the lung versus the secondary lymphoid organs, and suggest that a combination of effector functions is necessary for complete protection.

DISCUSSION

We have demonstrated that *in vivo*-generated, influenza virus-specific CD4 effectors confer protection to a lethal, highly pathogenic dose of PR8. CD4 cells displayed multifunctional and distinct properties in the DLN compared to the lung after sublethal infection. DLN CD4 cells maintained the ability to secrete IL-2 and proliferate upon restimulation, while lung resident CD4 cells secreted IFN-γ and IL-10. Lung CD4 cells, unlike DLN cells, expressed GrB, GrA, and perforin and could lyse peptide-pulsed target cells, albeit at lower levels than CD8 cells from the same anatomical site. Moreover, polyclonal and monoclonal populations of effector CD4 T cells from the lung exhibit substantial influenza virus-specific perforin-mediated cytolytic activity. Protection against lethal influenza virus infection was mediated by DLN and lung cells, and it appeared that optimum recovery from infection required the expression of IFN-γ and perforin. These data indicate that influenza virus infection induces differentiation of CD4 T cells with multiple functions which have a direct role in protection against lethal infection. Furthermore, these data should inform development of novel vaccine strategies that aim to induce multifunctional CD4 T cell responses against infection.

CD4 cells as direct mediators in protection against lethal influenza virus infection. It has been shown previously that CD4 T cell clones could confer protection against lethal H3N2 influenza virus infection and Th1 clones were more effective than Th2 clones in mediating survival (14). We have previously published that TCR Tg, HA-specific *in vitro*-generated CD4 effectors also protected mice from lethal infection with H1N1 PR8 in a B cell-independent manner (7), suggesting a direct effect of CD4 T cells in promoting survival. Because of the strong Th1 skewing in response to influenza virus infection, we reasoned that IFN-γ may be required for CD4 effector function *in vivo* and subsequent protection mediated by $CD4^+$ T cells. However, experiments in which IFN-γ-deficient cells were stimulated *in vitro* and investigated for their ability to promote survival demonstrated that IFN-γ was dispensable for protection (7, 15). In the current study, we wanted to extend our earlier findings and determine whether *in vivo*-generated CD4 effectors required IFN-γ during the priming phase for complete effector function and whether secretion of IFN-γ was important for protection. Not surprisingly, CD4 cells demonstrated the same level of proliferation, cytokine secretion, and ability to help the antibody response in WT mice as in IFN-$γ^{-/-}$ mice, indicating that IFN-γ is not required in the priming phase for helper functions. Further, IFN-γ did not impact the ability of

CD4 effectors to acquire cytolytic activity (Fig. 6B and C), consistent with our earlier findings with *in vitro*-generated effectors (7). In the absence of IFN-γ, CD4 cells produce higher levels of IL-17, possibly leading to pathogenic responses in lethally infected mice. This has been shown in mouse models of collagen-induced arthritis, where IFN-$γ^{-/-}$ C57BL/6 mice produce higher levels of IL-17 than their WT counterparts (10). Aberrant expression of IL-17 may lead to pathology in mice given $γ^{-/-}$ effectors *in vivo*, thus leading to more weight loss and a longer time to recovery (Fig. 6E). In a similar experimental system, CD4 memory cells generated by activation of $HA_{110-119}$ cells *in vitro* and transfer to BALB/c mice provided protection from lethal challenge in an IFN-γ-dependent manner (40). In recent work from the S. L. Swain lab, IFN-γ production by memory CD4 cells was shown to be required for protection when CD8 and B cells were absent but was not required in mice with the full complement of immune cells (K. McKinstry et al., submitted for publication). These results are in contrast to those of studies using IFN-$γ^{-/-}$ CD4 T cell clones (15) and our own work using *in vitro*-generated TCR Tg CD4 effectors (7), both of which demonstrate that IFN-γ has no effect on protection mediated by CD4 cells. Clearly, CD4 cells mediate protection against lethal influenza virus infection using a variety of mechanisms, and the relative contribution of IFN-γ in CD4-mediated protection may rely on the activation of concurrent CD8 and B cell responses to influenza virus.

CD4 CTLs in acute and chronic viral infection. This report is the first description of a bona fide CD4 killer cell isolated *ex vivo* in response to acute influenza virus infection in immunocompetent mice. Braciale's group has demonstrated CTL activity in CD4 cell clones generated in response to influenza virus (14), and our own data indicate that Th1-polarized, *in vitro*-generated CD4 effectors acquire perforin-mediated CTL activity (7, 8). CD4 CTLs have been described extensively in human subjects, and some groups hypothesize that differentiation to a cytolytic phenotype is the result of chronic infection or antigen stimulation (2, 44) and that the phenotype represents a CD4 effector cell at the latest stages of differentiation (1, 6, 33, 43). Here, we have demonstrated that an acute infection induces the differentiation of CD4 CTLs that reside in the lung, have an activated phenotype, and can kill peptide-pulsed targets directly *ex vivo* in a perforin-dependent manner. Reports of killing by CD4 CTLs directly *ex vivo* have been limited to CMV infection in human subjects (9, 44) and in mouse models of persistent infection, such as persistent infection with lymphocytic choriomeningitis virus (17) and mouse gamma herpesvirus 68 (34, 35). In an acute infection with influenza virus, we have demonstrated that a monoclonal population of HA-specific CD4 cells and a polyclonal population of CD4 effectors recognizing HA and NP peptides can lyse peptide-pulsed targets via a perforin-dependent mechanism. While CD4 effectors clearly utilize perforin and not FasL for killing directly *ex vivo*, the contribution of CD4-delivered perforin in weight loss and survival after lethal challenge was more obscure. In these experiments, total CD4 cells were transferred, but only the HNT-specific fraction was perforin deficient. Nonetheless, significant differences in weight loss were observed in mice that received perforin-deficient CD4 effectors compared to those that received WT effectors. More work needs to be done to further delineate the multiple mechanisms used by CD4 cells to mediate protection.

The physiological role of cytolytic CD4 cells has thus far not been elucidated; however, in many infections, CD4 cells have been

shown to contribute to viral clearance (5, 22, 24, 25). Certainly, during influenza virus infection, *in vitro*-generated CD4 CTLs and memory CD4 cells have been shown to lower viral titers (7, 40; McKinstry et al., submitted). Figure 3 demonstrates that influenza virus-infected epithelial cells can express class II molecules, thus serving as targets for CD4 CTLs. However, earlier reports suggest that class II recognition on epithelial cells was not required for influenza viral clearance by CD4 cells (42). This observation, coupled with results presented here, suggest that CD4 cells utilize many mechanisms that are not mutually exclusive to combat viral disease and promote survival against lethal infection. It remains to be determined whether *in vivo*-generated CD4 CTLs directly contribute to viral clearance in the primary response or whether these cells act to downregulate inflammation by killing APCs in the lung, as has been proposed in a tumor immunity model (4).

An intriguing question is whether CD4 CTLs develop into memory cells and what the contribution of perforin may be in this situation. Teijaro et al. recently reported that lung resident CD4 memory cells were more effective than splenic memory cells at reducing viral titers and promoting recovery to lethal infection (39). This suggests that a proportion of CD4 effectors that migrate to the lung may remain memory cells capable of CTL activity upon restimulation. In other yet unpublished work, McKinstry et al. demonstrated a role for CD4 memory cell-derived perforin in driving influenza virus escape mutants in a model of lethal infection in B cell-deficient mice (McKinstry et al., submitted). The role of CD4 CTL in the memory response has yet to be elucidated, and whether CD4 memory cells reexpress cytolytic proteins upon restimulation will be important for vaccine design.

Signals important for CD4 CTL differentiation. The signals required for differentiation of CD4 CTLs have not been clearly identified, especially in response to infection *in vivo*. A straightforward hypothesis posits that CD4 CTLs are a further differentiation state of the Th1 phenotype. Our data seem to support this, as transcriptional profiles of CD4 CTLs in the lung show high levels of T-bet expression (Fig. 4A) and low levels of Eomes, a transcription factor important in CD8 CTL differentiation. This is in contrast to a recent report that demonstrates that Eomes is required *in vivo* for CD4 CTL generation; however, that study used a model of dual costimulation through CD134 and CD137 to differentiate CD4 CTLs for use in tumor immunotherapy (29). The role of Eomes in driving CD4 CTLs in the response to an acute infection such as one with influenza virus has yet to be identified. Separate studies from our laboratory using *in vitro*-generated CD4 effectors polarized to different subsets have shown that IFN-γ or IL-12 is not necessary for differentiation to the cytolytic phenotype and IL-4 can inhibit generation of CD4 CTLs, suggesting that CD4 CTLs differentiate independently of Th1 or Th2 subset polarization (8). Studies are under way to determine if T-bet or Eomes is necessary for CD4 CTL development in response to influenza virus infection or whether CD4 CTLs express unique transcription factors that may delineate a novel CD4 T cell subset. In support of a separate lineage for CD4 CTLs, preliminary data from our lab indicate that not all cells expressing CD107a, a marker of degranulation, express IFN-γ. In fact, the proportion of CD107a$^+$ cells that also express IFN-γ is much lower for CD4 cells (30%) than the proportion of CD107a$^+$ cells that express IFN-γ in CD8 cells (70%) (D. M. Brown et al., unpublished observation). Ongoing work in our laboratory aims to identify the signals required for direct differentiation to CD4 CTLs. Given the lack of CTL markers

in effectors generated from the DLN compared to CD4 cells from the lung, we hypothesize that a secondary signal at the site of infection may be responsible for further CD4 CTL differentiation. Whether this signal is inflammatory or antigen specific is a subject of further work from our lab.

Vaccine strategies that target CD4 CTLs. The expanding body of literature concerning the appearance of CD4 CTLs in various viral diseases and malignancies underscores the need to develop alternative vaccine strategies that target CD4 CTLs (as well as multifunctional CD4 cells) to the site of infection (6, 33, 37, 43). Data from Seder's group have shown that vaccine-induced, multifunctional CD4 cells expressing IL-2, IFN-γ, and TNF-α were most effective at protection against *Leishmania major* infection (12). Moreover, an adjuvant that mimicked live infection (i.e., CpG oligonucleotide) was the best at inducing the multifunctional CD4 T cell population. Encouraging data in seasonal influenza virus vaccine trials in the elderly suggest that the appearance of GrB-positive CD4 cells is a better correlate of protection than the antibody response (21). In addition, FluMist live attenuated vaccine induced a population of memory CD4 cells that were important for lowering viral titers in a mouse model of 2009 H1N1 infection (36). These reports all highlight the need to develop effective vaccines for infections that escape the antibody response and induce multifunctional cytokine-secreting CD4 T cells with cytotoxic ability as well as helper activities.

REFERENCES

1. **Appay V.** 2004. The physiological role of cytotoxic CD4(+) T-cells: the holy grail? Clin. Exp. Immunol. **138**:10–13.
2. **Appay V, et al.** 2002. Characterization of CD4(+) CTLs ex vivo. J. Immunol. **168**:5954–5958.
3. **Baumgarth N, Kelso A.** 1996. In vivo blockade of gamma interferon affects the influenza virus-induced humoral and the local cellular immune response in lung tissue. J. Virol. **70**:4411–4418.
4. **Boissonnas A, et al.** 2010. Foxp3+ T cells induce perforin-dependent dendritic cell death in tumor-draining lymph nodes. Immunity **32**:266–278.
5. **Brien JD, Uhrlaub JL, Nikolich-Zugich J.** 2008. West Nile virus-specific CD4 T cells exhibit direct antiviral cytokine secretion and cytotoxicity and are sufficient for antiviral protection. J. Immunol. **181**:8568–8575.
6. **Brown DM.** 2010. Cytolytic CD4 cells: direct mediators in infectious disease and malignancy. Cell. Immunol. **262**:89–95.
7. **Brown DM, Dilzer AM, Meents DL, Swain SL.** 2006. CD4 T cell-mediated protection from lethal influenza: perforin and antibody-mediated mechanisms give a one-two punch. J. Immunol. **177**:2888–2898.
8. **Brown DM, Kamperschroer C, Dilzer AM, Roberts DM, Swain SL.** 2009. IL-2 and antigen dose differentially regulate perforin- and FasL-mediated cytolytic activity in antigen specific CD4+ T cells. Cell. Immunol. **257**:69–79.
9. **Casazza JP, et al.** 2006. Acquisition of direct antiviral effector functions by CMV-specific CD4+ T lymphocytes with cellular maturation. J. Exp. Med. **203**:2865–2877.
10. **Chu CQ, Swart D, Alcorn D, Tocker J, Elkon KB.** 2007. Interferon-

gamma regulates susceptibility to collagen-induced arthritis through suppression of interleukin-17. Arthritis Rheum. **56**:1145–1151.

11. **Cruz A, et al.** 2006. Cutting edge: IFN-gamma regulates the induction and expansion of IL-17-producing CD4 T cells during mycobacterial infection. J. Immunol. **177**:1416–1420.

12. **Darrah PA, et al.** 2007. Multifunctional TH1 cells define a correlate of vaccine-mediated protection against Leishmania major. Nat. Med. **13**:843–850.

13. **Freches D, et al.** 2011. Increased pulmonary tumor necrosis factor alpha, interleukin-6 (IL-6), and IL-17A responses compensate for decreased gamma interferon production in anti-IL-12 autovaccine-treated, Mycobacterium bovis BCG-vaccinated mice. Clin. Vaccine Immunol. **18**:95–104.

14. **Graham MB, Braciale VL, Braciale TJ.** 1994. Influenza virus-specific CD4+ T helper type 2 T lymphocytes do not promote recovery from experimental virus infection. J. Exp. Med. **180**:1273–1282.

15. **Graham MB, et al.** 1993. Response to influenza infection in mice with a targeted disruption in the interferon gamma gene. J. Exp. Med. **178**:1725–1732.

16. **Jelley-Gibbs DM, et al.** 2005. Unexpected prolonged presentation of influenza antigens promotes CD4 T cell memory generation. J. Exp. Med. **202**:697–706.

17. **Jellison ER, Kim SK, Welsh RM.** 2005. Cutting edge: MHC class II-restricted killing in vivo during viral infection. J. Immunol. **174**:614–618.

18. **Kamperschroer C, Dibble JP, Meents DL, Schwartzberg PL, Swain SL.** 2006. SAP is required for Th cell function and for immunity to influenza. J. Immunol. **177**:5317–5327.

19. **Matzinger P.** 1991. The JAM test. A simple assay for DNA fragmentation and cell death. J. Immunol. Methods **145**:185–192.

20. **Mayer KD, et al.** 2005. The functional heterogeneity of type 1 effector T cells in response to infection is related to the potential for IFN-gamma production. J. Immunol. **174**:7732–7739.

21. **McElhaney JE, et al.** 2006. T cell responses are better correlates of vaccine protection in the elderly. J. Immunol. **176**:6333–6339.

22. **Mohindru M, Kang B, Kim BS.** 2006. Initial capsid-specific CD4(+) T cell responses protect against Theiler's murine encephalomyelitis virus-induced demyelinating disease. Eur. J. Immunol. **36**:2106–2115.

23. **Mozdzanowska K, Furchner M, Maiese K, Gerhard W.** 1997. CD4+ T cells are ineffective in clearing a pulmonary infection with influenza type A virus in the absence of B cells. Virology **239**:217–225.

24. **Nikiforow S, Bottomly K, Miller G, Munz C.** 2003. Cytolytic CD4(+)-T-cell clones reactive to EBNA1 inhibit Epstein-Barr virus-induced B-cell proliferation. J. Virol. **77**:12088–12104.

25. **Norris PJ, et al.** 2004. Beyond help: direct effector functions of human immunodeficiency virus type 1-specific CD4(+) T cells. J. Virol. **78**:8844–8851.

26. **Pearce EL, et al.** 2003. Control of effector CD8+ T cell function by the transcription factor eomesodermin. Science **302**:1041–1043.

27. **Pipkin ME, Rao A, Lichtenheld MG.** 2010. The transcriptional control of the perforin locus. Immunol. Rev. **235**:55–72.

28. **Powell TJ, et al.** 2004. CD8+ T cells responding to influenza infection reach and persist at higher numbers than CD4+ T cells independently of precursor frequency. Clin. Immunol. **113**:89–100.

29. **Qui HZ, et al.** 2011. CD134 plus CD137 dual costimulation induces eomesodermin in CD4 T cells to program cytotoxic Th1 differentiation. J. Immunol. **187**:3555–3564.

30. **Ramakrishna C, Stohlman SA, Atkinson RD, Shlomchik MJ, Bergmann CC.** 2002. Mechanisms of central nervous system viral persistence: the critical role of antibody and B cells. J. Immunol. **168**:1204–1211.

31. **Roman E, et al.** 2002. CD4 effector T cell subsets in the response to influenza: heterogeneity, migration, and function. J. Exp. Med. **196**:957–968.

32. **Scott B, et al.** 1994. A role for non MHC genetic polymorphism in susceptibility to spontaneous autoimmunity. Immunity **1**:73–82.

33. **Soghoian DZ, Streeck H.** 2010. Cytolytic CD4(+) T cells in viral immunity. Expert Rev. Vaccines **9**:1453–1463.

34. **Stuller KA, Cush SS, Flano E.** 2010. Persistent gamma-herpesvirus infection induces a CD4 T cell response containing functionally distinct effector populations. J. Immunol. **184**:3850–3856.

35. **Stuller KA, Flano E.** 2009. CD4 T cells mediate killing during persistent gammaherpesvirus 68 infection. J. Virol. **83**:4700–4703.

36. **Sun K, Ye J, Perez DR, Metzger DW.** 2011. Seasonal FluMist vaccination induces cross-reactive T cell immunity against H1N1 (2009) influenza and secondary bacterial infections. J. Immunol. **186**:987–993.

37. **Swain SL, McKinstry KK, Strutt TM.** 2012. Expanding roles for CD4 T cells in immunity to viruses. Nat. Rev. Immunol. **12**:136–148.

38. **Taubenberger JK, Kash JC.** 2010. Influenza virus evolution, host adaptation, and pandemic formation. Cell Host Microbe **7**:440–451.

39. **Teijaro JR, et al.** 2011. Cutting edge: tissue-retentive lung memory CD4 T cells mediate optimal protection to respiratory virus infection. J. Immunol. **187**:5510–5514.

40. **Teijaro JR, Verhoeven D, Page CA, Turner D, Farber DL.** 2010. Memory CD4 T cells direct protective responses to influenza virus in the lungs through helper-independent mechanisms. J. Virol. **84**:9217–9226.

41. **Topham DJ, Tripp RA, Doherty PC.** 1997. CD8+ T cells clear influenza virus by perforin or Fas-dependent processes. J. Immunol. **159**:5197–5200.

42. **Topham DJ, Tripp RA, Sarawar SR, Sangster MY, Doherty PC.** 1996. Immune CD4+ T cells promote the clearance of influenza virus from major histocompatibility complex class II$^{-/-}$ respiratory epithelium. J. Virol. **70**:1288–1291.

43. **van de Berg PJ, van Leeuwen EM, ten Berge IJ, van Lier R.** 2008. Cytotoxic human CD4(+) T cells. Curr. Opin. Immunol. **20**:339–343.

44. **van Leeuwen EM, Remmerswaal EB, Heemskerk MH, ten Berge IJ, van Lier RA.** 2006. Strong selection of virus-specific cytotoxic CD4+ T-cell clones during primary human cytomegalovirus infection. Blood **108**:3121–3127.

45. **Wang ZE, et al.** 1994. Interferon gamma-independent effects of interleukin 12 administered during acute or established infection due to Leishmania major. Proc. Natl. Acad. Sci. U. S. A. **91**:12932–12936.